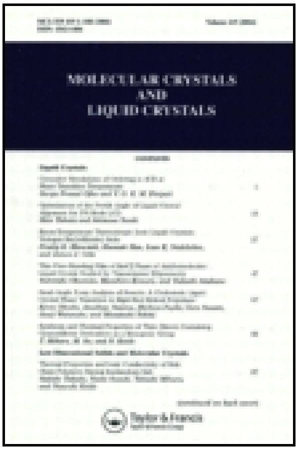

Molecular Crystals and Liquid Crystals Science and Technology. Section A. Molecular Crystals and Liquid Crystals

Publication details, including instructions for authors and subscription information:
http://www.tandfonline.com/loi/gmcl19

Structure of the Smectic B Phase Formed by Linear and Branched Perfluoroalkyl-Alkanes

F. G. Tournilhac [a] , P. Bassoul [a] & R. Cortès [b]

[a] Chimie Inorganique et Matériaux Moléculaires (CNRS ESA 7071), Ecole Supérieure de Physique et de Chimie Industrielles, 10 rue Vauquelin, 75231, Paris, Cedex 05, France

[b] Physique des Liquides et Electrochimie (CNRS UPR 15), Université Pierre et Marie Curie, 4 place Jussieu, 75252, Paris, Cedex 05, France

To cite this article: F. G. Tournilhac, P. Bassoul & R. Cortès (2001): Structure of the Smectic B Phase Formed by Linear and Branched Perfluoroalkyl-Alkanes, Molecular Crystals and Liquid Crystals Science and Technology. Section A. Molecular Crystals and Liquid Crystals, 362:1, 45-65

To link to this article: http://dx.doi.org/10.1080/10587250108025759

Mol. Cryst. Liq. Cryst., Vol. 362, pp. 45-65
Reprints available directly from the publisher
Photocopying permitted by license only

Published by license under the
Gordon and Breach Science Publishers imprint,
a member of the Taylor & Francis Group.
Printed in the USA

Structure of the Smectic B Phase Formed by Linear and Branched Perfluoroalkyl-Alkanes*

F.G. TOURNILHAC[a]†, P. BASSOUL[a] and R. CORTÈS[b]

[a]*Chimie Inorganique et Matériaux Moléculaires (CNRS ESA 7071), Ecole Supérieure de Physique et de Chimie Industrielles, 10 rue Vauquelin, 75231 Paris Cedex 05, France and* [b]*Physique des Liquides et Electrochimie (CNRS UPR 15), Université Pierre et Marie Curie, 4 place Jussieu, 75252 Paris Cedex 05, France*

The structure of the smectic B phase formed by perfluorodecylalkanes has been analyzed through the synthesis of three molecules and a careful investigation of their mesophases. Molecules with C_8, C_{10} and a branched C_{11} alkyl chain were considered. The structure factor analysis of 00*l* reflexions is consistent with the picture of alternating electron rich and electron poor sublayers. A structural model with segregated perfluoroalkyl chains in the middle of the layer and disordered alkyl chains on each sides is proposed. This model is discussed in terms of space filling arguments: chain lengths, cross section compatibility in the layer and compactness. Infrared dichroic ratios of the CH_2 and CF_2 stretching modes confirm that perfluoroalkyl subunits are perpendicular to the S_B layer while alkyl ones, in a quasi molten state, fill the remaining layer space.

1. INTRODUCTION

Perfluorodecyl-decane‡ is a liquid crystalline molecule of rather unusual anatomy since it doesn't contain any benzenic or alicyclic ring. Nevertheless, it displays the smectic B mesophase (S_B) between 38 and 61 °C. This peculiarity was first investigated by A. Skoulios and coworkers [1] who recognized the amphiphilic constitution of the molecule to be responsible of the mesomorphic properties. The perfluoroalkyl and alkyl fragments are both highly hydrophobic, almost unpolar and unable to associate through hydrogen bonds, but the two fragments have quite different values of their molecular polarizability which is sufficient to confer a certain degree of incompatibility between them [2]. In fur-

---

* This work was presented in the International Forum on Chemistry and Characterization of Mesophase Materials (Bayreuth 1998)

† Corresponding author.

‡ 1,1,1,2,2,3,3,4,4,5,5,6,6,7,7,8,8,9,9,10,10-henicosafluoro-eicosane

ther studies, perfluoroalkyl chains were often incorporated in new mesogenic molecules [3–6] and polymers [7–10]; polyphilic molecules, in particular [11] are based on the segregating properties of perfluoroalkyl chains towards alkyl and biphenyl moieties. Meanwhile, in the structural study of perfluorodecyl-decane published by Viney et al [12], there is no evidence of any segregating property.

In this paper, we report the synthesis of three perfluorodecyl-alkane molecules and carefully examine the structural features of their smectic B phase. The analysis of X-ray diffraction intensities permits to determine the location of each molecular fragment inside the smectic layers. A structural model with segregated alkyl and perfluoroalkyl chains is proposed. Space filling requirements lead to different conformations for alkyl and perfluoroalkyl chains which is confirmed by IR dichroism measurements.

2. MATERIALS

Perfluorooctyldecane, **4a** and perfluorodecyldecane, **4b** (scheme 1) were prepared by 1,2 addition of perfluorodecyl iodide, **1** on the double bond of 1-octene, **2a** or 1-decene, **2b** followed by Zn/H$^+$ reduction [12] (scheme 1).

SCHEME 1

Compound **9** with a branched alkyl chain was synthesized similarly from the branched chain alkene **7** (scheme 2): Allylmagnesium bromide, **5** was reacted with 2-ethyl-1-hexyl-bromide, **6** in the presence of copper (I) bromide [13], giving 5-ethyl-non-1-ene, **7**. Alternatively, 2-ethyl-1-hexyl-magnesium bromide was reacted in the same way with allyl bromide but the compound therebye obtained was difficult to separate form unreacted 2-ethyl-1-hexylbromide. Compound **7** was reacted with perfluorodecyl iodide, **1** in the presence of peroxides [14–16]. The addition product, **8** was then reduced by Zn/HCl and 15-ethyl-henicosafluoro-nonadecane, **9** was obtained as a racemic mixture.

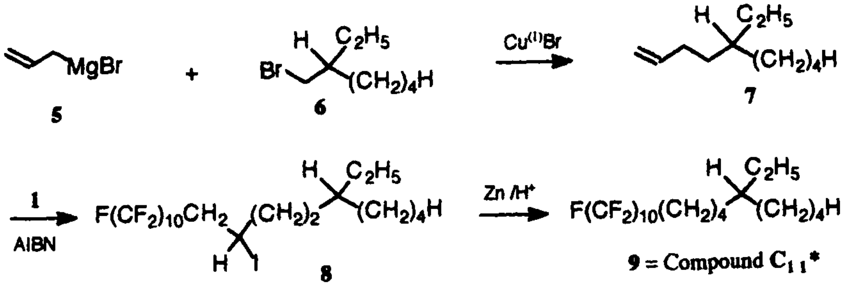

SCHEME 2

TABLE I Transition temperatures, enthalpies, observed Bragg spacings and calculated cell parameters of the three investigated compounds

Compound	C_8	C_{10}	C_{11}^*
$T_{K\text{-}Sm}$ (°C)	26.2	35.2	
ΔH (kJ/mol)	3.7	2.5	
$T_{Sm\text{-}I}$ (°C)	56.2	62.2	32.7
ΔH (kJ/mol)	20.7	23.6	14.5
Reflexions: 2π/q (Å)			
001	24.78	27.60	26.68
002	12.63	13.72	13.46
003	8.36	9.16	8.86
004			6.73
100	9.65		9.87
200 = 110	4.81	4.73	4.93
201 = 111			4.86
020	2.78		2.85
021			2.83
022			2.79
400	2.41		2.47
401			2.46
halo	5.2	5.2	5.2
Orthorhombic cell (Å)			
a	9.62	9.46	9.86
b	5.55	5.46	5.69
c	25.17	27.51	26.84

In the following, compounds **4a, 4b** and **9** will be labelled with the number of carbon atoms in the alkyl chain: C_8, C_{10} and C_{11}^* respectively. Transition temperatures of C_8 and C_{10} (table I) detected by DSC (+/- 5°C/mn) were very close to previously reported ones [1,12]. Compound C_{11}^* is mesomorphic at room temperature and turns to the isotropic liquid at 32.7°C (table I). The optical textures of the mesophase are presented in plate 1. Elongated birefringent platelets appear on cooling from the isotropic phase. The pictures are very similar to those reported for C_{10} [1,12] in the smectic B phase.

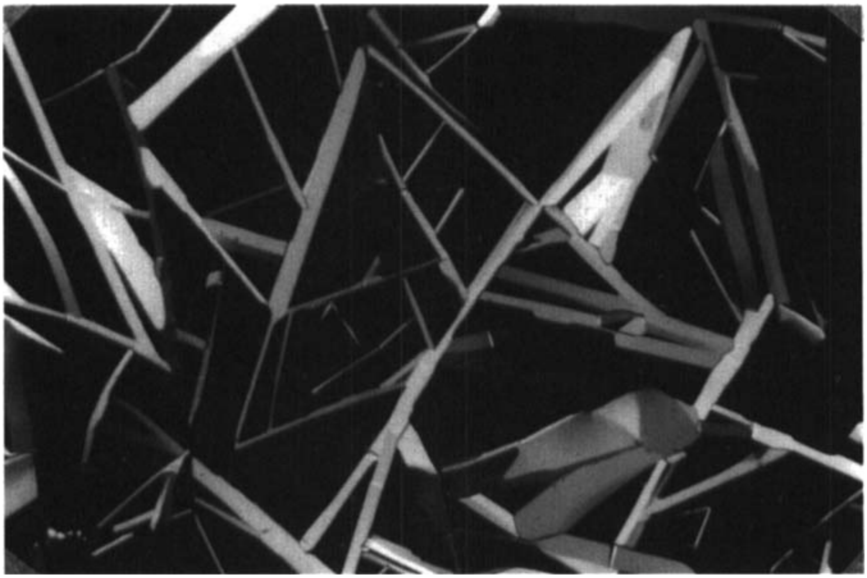

PLATE 1 The optical texture of compound C_{11}^* at room temperature. The sample was cooled down from its isotropic phase. Crossed polarizers, full range = 1 mm

3. X-RAY STUDY OF THE MESOPHASES

3.1 Method

X-ray diffraction experiments were carried out from powder samples using three different setups.

i) The overall shape of the diffraction figures were obtained with a Debye-Scherrer camera operating with the CuKα radiation (figure 1 and table I).

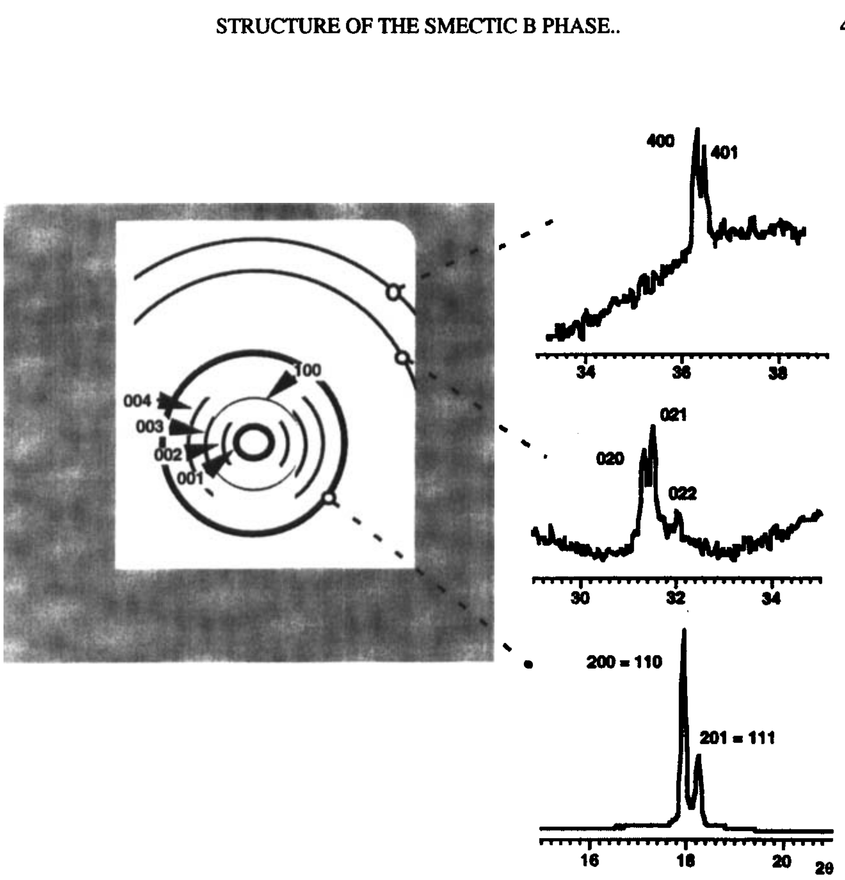

FIGURE 1 The Debye-Scherrer picture obtained from compound C_{11}^*. The sample displays a spontaneous partial orientation in a vertical 1 mm Lindemann tube. The inserts show the resolution of *hk*0 and *hkl* lines (see **3.1** for experimental details)

ii) Accurate measures of the layer spacing of C_{10} were obtained using the $CuK\alpha_1$ radiation on a small angle bench equipped with a double monochromator and allowing independant motions of the sample and of the detector. A powder filled capillary was kept immobile and its temperature was regulated with an accuracy of +/- 0.5°C, the beam section was 50 μm × 1 mm, diffracted beams were collected in the meridian plane through a slit of similar shape. The experimental resolution in these conditions was 0.5 mRad (FWHM) on 2θ. This method permitted to measure the layer spacing with an accuracy of 0.1 Å (table I).

iii) The angular splitting of very close *hk*0 and *hkl* lines was measured for C_{11}^* (inserts of figure 1 and table I) using a CPS 120 Inel position sensitive detector affording a resolution of 22 mRad (FWHM).

3.2 Results

Diffraction data of C_8, C_{10} and C_{11}^* are collected in table I and figure 1. At narrow angles, all investigated compounds display a series of 00*l* Bragg reflexions indicating a layered arrangement. The corresponding c parameter increases with the number of carbon atoms in the main chain. At large angles, *hk*0 and *hkl* reflexions could be recognized (figure 1). In C_8, C_{10} and C_{11}^*, the *in-plane hk*0 reflexions occur at very close angles indicating that the compounds have approximately the same S_B structure. Therefore, the same structural model should be made for compounds with branched chains or linear chains.

The main difference between the diffraction patterns of investigated compounds is the relative importance of reflexions intensities with respect to the background. Compound C_{11}^*, which presents the highest number of *in-plane* reflexions may be indexed with a rectangular unit cell of parameters a= 9.86, b= 5.69 Å. 0*k*0 lines, with *k* odd were not encountered, indicating a glide symmetry element. Two different ^{2}D spacegroups are compatible with this extinction law: p2mg and pg. Their symmetry elements are drawn in figure 2.

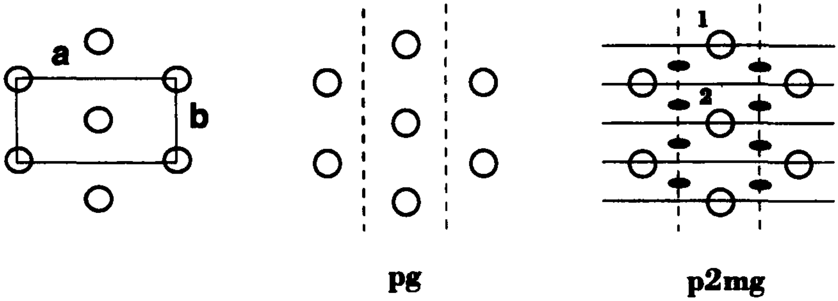

FIGURE 2 Symmetry elements in the two dimensional spacegroups pg and p2mg. Molecules are centered on a hexagonal array

The presence of *hkl* lines was checked only for C_{11}^* using the position sensitive detector. These lines indicate positional correlations between the smectic planes. The same device was not able to separate 110 and 020 lines ($2\pi/q = 4.93$ Å), their coincidence corresponds to a hexagonal array ($a/b = \sqrt{3}$) but the presence of the 100 line is only compatible with a ^{3}D orthorhombic cell whose symmetry is lower than the hexagonal one.

3.3 Interlayer spacings

The geometrical characteristics of the various chemical groups present in the molecule can be obtained from the literature. The length of $F(CF_2)_n(CH_2)_mH$

molecules in their fully extended conformation can be calculated through the formula:

$$\begin{aligned} l = {} & r_F + l_{CF} \sin \frac{\widehat{FCC}}{2} + \left(n - \frac{1}{2}\right) l^F_{CC} \sin \frac{\widehat{CCC_F}}{2} \\ & + \left(m - \frac{1}{2}\right) l^H_{CC} \sin \frac{\widehat{CCC_H}}{2} + l_{CH} \sin \frac{\widehat{CCH}}{2} + r_H \end{aligned} \qquad (1)$$

Where l^F_{CC}, l_{CF}, l_{CH}, $\widehat{HCC}$, $\widehat{FCC}$ and $\widehat{CCC_i}$ are the typical bond lengths and bond angles in hydrocarbons and fluorocarbons and r_i the Van der Waals radii of organic hydrogen and fluorine. The length of the CF_2-CH_2 bridge is approximated by the mean of CH_2-CH_2 and CF_2-CF_2 bonds. Using tabulated numerical values [17–18], the full length becomes:

$$l = 1.306n + 1.265m + 3.26 \qquad (2)$$

The calculated lengths of compounds C_8 and C_{10} are presented in table II. In the case of C_{11}^*, m is the number of carbon atoms in the main hydrocarbon chain (m=9).

TABLE II Calculated molecular length, l and molecular volume, V_K of investigated compounds, abc/Z is the volume per molecule and χ the compactness in the smectic B phase. See formulas (2, 3, 4)

	C_8	C_{10}	C_{11}^*
l(Å)	26.5	29.0	27.7
V_K (Å^3)	362	398	416
abc/Z (Å^3)	672	710	752
χ	0.54	0.56	0.55

The volume of the molecules, V_K, defined as the envelope of interpenetrating Van der Waals spheres was calculated by the Kitaigorodski method [19] using the Fastvol module in Moldraw [20]. For linear $F(CF_2)_n$-$(CH_2)_mH$ molecules, this volume in Å^3 was found equal to:

$$V_K = 21.5\ n + 17.1\ m + 12 \qquad (3)$$

Formula (3) is also valid for C_{11}^* provided that m is the total number of carbon atoms in the branched hydrocarbon chain (m=11 in this case), V_k values are presented in table II. In their investigation of perfluoroalkyl alkanes, Mita et al. [21] found a c/l ratio close to unity in the whole homological series: $F(CF_2)_{10}$-$(CH_2)_nH$, with n the number of carbon atoms in the alkyl chain ranging from 6 to 10. In the following discussion, we will show that the comparison between the interlayer distance, c and the molecular length, l may give a misleading view of the molecular packing in the layers.

The C_{10} molecule in its fully elongated conformation has a length l = 29.0 Å. At first sight, this value is close to the measured interlayer distance, 27.5 Å. The difference between the two values may be accounted for by a small tilt angle θ~16° or a partially disordered conformation of the chains. Considering that the perfluoroalkyl and alkyl fragment have approximately the same length but not the same cross section, a model with interdigitation of strectched alkyl and perfluoroalkyl stems seems to be the most satisfactory from the close packing standpoint (model **I** in figure 3).

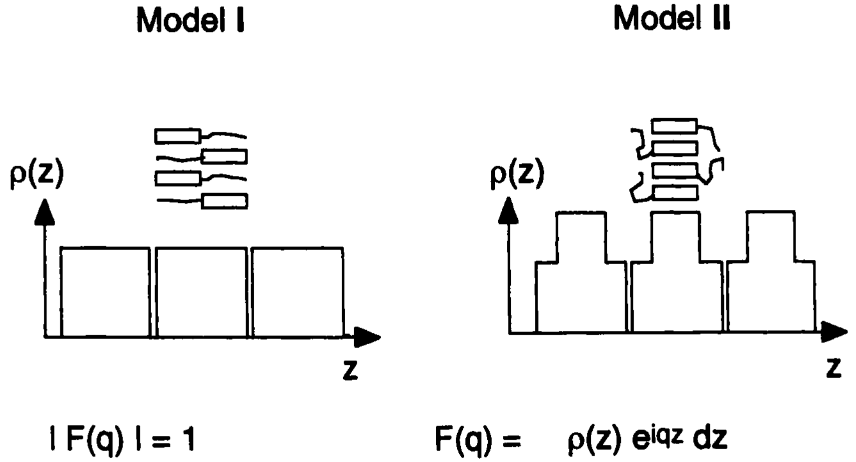

FIGURE 3 Schematic representation of the two structural models for the S_B phase and corresponding electron density profiles ρ(z) used to calculate $F(q_{00l})$

The perfluoroalkyl stem in C_8 is longer than its alkyl part. With this compound, the argument of close packing with straight antiparallel molecules breaks down. The antiparallel packing of model **I** would imply the overlap of bulky perfluorinated chains in the middle of the layer without any profit in terms of density. Nevertheless, the c/l ratio is again close to unity (tables I and II).

Considering now compound C_{11}^* with a branched chain, it is expected that its protruding ethyl group prevents neighbouring molecules to stack parallel to each other. Model **I** with antiparallel stretched molecules is therefore also highly unlikely with this compound.

3.4 In-plane order

The area per molecule occupied in the smectic layer can be compared to those of well known arrangements of alkyl and perfluoroalkyl chains. The typical lattice parameters of alkanes and perfluoroalkanes in their different allotropic forms are collected in table III. In the gel phase of concentrated soap solutions [22] alkyl chains form a rectangular arrangement with an area of 18.5 Å^2 per molecule. On elevating the temperature, a hexagonal packing appears, corresponding to a molecular area of 19.4 Å^2. Concerning the perfluoroalkyl chains, the minimum of intramolecular potential corresponds to an helical conformation with a pitch of 13 CF_2 units [23]. Perfluoroalkyl compounds crystallize in a hexagonal cell of 27.6 Å^2 area [24,25]. From crystal data relative to short chain fluorinated materials [26] we also found that the perfluoroalkyl chain in the *all-trans* conformation can also organize in an oblique arrangement with an area of 23.8 Å^2.

As seen in table III, the cell dimensions (in the hexagonal cell description) of C_8, C_{10} and C_{11}^* can be compared to those of perfluoroalkyl chains in the hexagonal form but are incompatible with those of all other arrangements. On the other hand, it is worth noting that the cell parameters of C_{11}^* are only slightly larger than those of C_8 and C_{10} despite the presence of the lateral ethyl group. It is therefore evident that the cell dimensions are mainly determined by the close packing of perfluoroalkyl chains. Then, stretched perfluoroalkyl chains, with a hexagonal *in-plane* ordering may be supposed to form a segregated sublayer in the centre of each smectic lamella (model II in figure 3). The occupied area per molecule is 27 Å^2. With alternating alkyl chains the space available for each of them is 54 Å^2, twice the typical dimensions of alkyl chains. These latter must take a disordered conformation in order to fill the remaining space on either sides of the perfluoroalkyl sublayer (figure 4).

TABLE III Typical values of the lattice parameters encountered in crystalline alkyl and perfluoroalkyl compounds (see text for references). Experimental hexagonal arrays of C_8, C_{10} and C_{11}^*. s: cross section per molecule perpendicular to the chain axis

	a(Å)	*b(Å)*	*γ(°)*	*Z*	*s(Å²)*
Alkanes					
rectangular	7.6	4.87	90	2	18.5
hexagonal	4.73		120	1	19.4
Perfluoroalkanes					
oblique	6.18	3.86	94	2	23.8
hexagonal	5.65		120	1	27.6
Experimental					
C_8	5.55		120	1	26.7
C_{10}	5.46		120	1	25.8
C_{11}^*	5.69		120	1	28.0

These assumptions can also be tested on the basis of volume considerations. Knowing the hexagonal parameter, the interlayer spacing and the thickness of the central sublayer – equal to the length of the stretched perfluorodecyl unit – one can calculate the volume available for each alkyl chain. For compound **C_{10}**, we found a value of 301 $Å^3$, equal to the molecular volume of $C_{10}H_{21}$ in the liquid state [17]. The presence of alkyl chains in a liquidlike conformation is also in good agreement with the halo observed around $2\pi/q = 5.2$ Å (table I). In order to evaluate the degree of disorder existing in the mesophase, we calculate its compactness χ:

$$\chi = ZV_K/abc \qquad (4)$$

where Z is the number of molecules in the unit cell, a, b, c, the lattice parameters and V_K the molecular volume already defined (3). $Z = 2$ leads to a realistic χ value ranging from 0.54 to 0.56 for studied molecules (table II). The same calculation effected on a series of eight polyfluorinated compounds of known crystalline structure [26] leads to significantly higher figures (from 0.61 to 0.66).

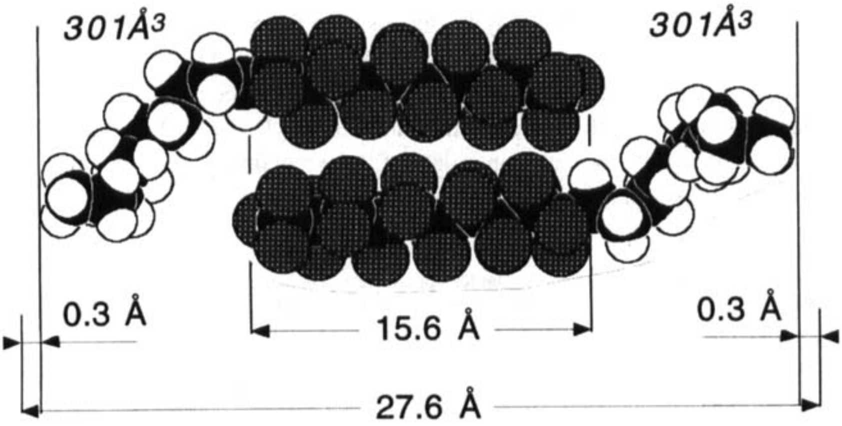

FIGURE 4 Segregated arrangement of molecules in model II. The volume per alkyl chain, 301 $Å^3$ is deduced from experimental lattice parameters and calculated perfluoroalkyl length. An interlayer gap of 0.6 Å is assumed

In the case of C_{11}^* with branched chain, model **II** allows the bulky ethyl group to be accomodated in the region of disordered alkyl chains. Actually, the compactness is the same for branched and nonbranched molecules (table II). Similar observations were made by Höpken et al. on molecules with a pendent methyl group in the alkyl chain [27].

3.5 Structure factor analysis

Relative intensities of $00l$ reflexions in compound C_{10} (table IV) were estimated by measuring the optical density of Debye-Scherrer films. They can be related to the one-dimensional structure factor $|F(q_{00l})|$ of models through the formula: [28]

$$I(q_{00l}) \sim \frac{1}{q^2_{00l}} |F(q_{00l})|^2 \exp(-\sigma^2 q^2_{00l}) \qquad (5)$$

$1/q^2_{00l}$ is the relevant Lorenz correction factor at small diffraction angles and σ the Debye-Waller coefficient which accounts for positional fluctuations in the smectic phase. In the case of rodlike mesogens, the electronic density may be supposed uniform within the layers and equal to zero in the interlayer gaps. In the limit case of infinitely thin interfaces, all $|F(q_{00l})|$ factors are equal to unity. The same form factor may be applied to describe the interdigitated alkyl and perfluoroalkyl moieties of model **I** (figure 3). Since these two fragments have approximately the same length in perfluorodecyl decane, their overlap inside the layer leads to a constant electron density along the layer normal. In the frame of this approximation, since $|F(q_{00l})| = 1$ whatever l, $\mathrm{Ln}(I \times q^2)$ ought to decrease linearly with q^2. From experimental data, I_{003} is too strong to fit such a law. Model **II** in contrast, corresponds to a crenel shaped electron density profile (figure 3) and the $00l$ reflexion intensities calculated from formula 5 match those experimentally observed for C_{10} (table IV).

TABLE IV Comparison between measured reflexion intensities of C_{10} and those calculated from model II

I(hkl)	*001*	*002*	*003*	*004*
exp	100	1.52	0.53	0
calc	100	1.44	0.45	0.08

As already mentioned, the observed *hk*0 lines are compatible with two different ^{2}D spacegroups: pg and p2mg (figure 2). The p2mg group possess mirror planes perpendicular to the glide plane. In order to keep a hexagonal array in p2mg, the molecules must be located on the mirror planes. The molecule itself should therefore possess a symmetry plane which is precisely not the case of C_{11}^*, a mixture of chiral enantiomers. C_8 and C_{10} do possess a symmetry mirror in the *all-trans* conformation but this situation does not correspond to a minimum of the intramolecular potential [18]. For these reasons, we retain pg as the ^{2}D spacegroup. A static view of the packing, compatible with this group is a rectangular herringbone arrangement of perfluoroalkyl chains with a single helicoidal axis 2_1 perpendicular to the chain axis (figure 5). The two molecules in the unit cell have up and down alternating alkyl chains and the ^{3}D spacegroup of the structural model is P_{2_1}.

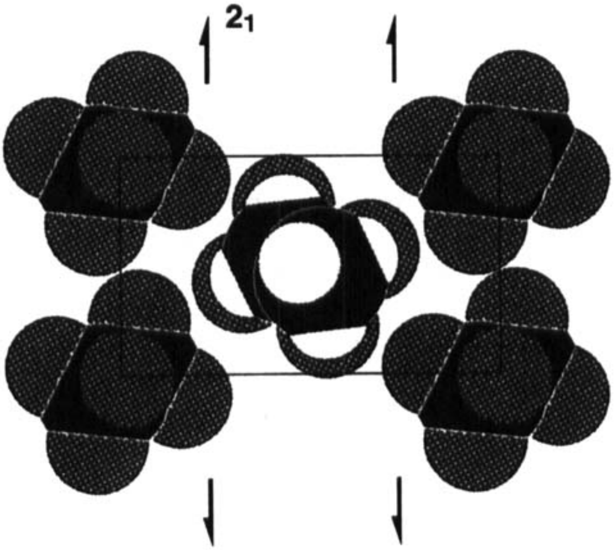

FIGURE 5 Schematic view showing the herringbone arrangement of the perfluoroalkyl chains. The symmetry elements of the two dimensional spacegroup pg are replaced by a two fold helical axis in the ^{3}D spacegroup P_{2_1}. Alkyl chains are pointing up and down alternatively (See Color Plate I at the back of this issue)

4. INFRARED DICHROISM

4.1 Method

Fourier transform infrared spectra were recorded in the 4000–400 cm^{-1} range from homeotropically oriented specimens of compound C_{10}. The material was deposited as a thin film onto the surface of a KBr window and cooled down from its isotropic phase. Polished potassium bromide crystals proved to be more efficient than freshly cleaved ones for obtaining the homeotropic texture. Due to the absence of the nematic and smectic A phases, we experienced difficulties to obtain large monodomains; a sample showing the homeotropic texture over more than 90 percent of its surface was investigated after masking the birefringent areas.

Dichroic ratios were obtained by comparing the absorbance of unpolarized light (optical density) in the isotropic phase, D_i with that of the homeotropically oriented smectic phase, D_h. According to the previously described method [29],

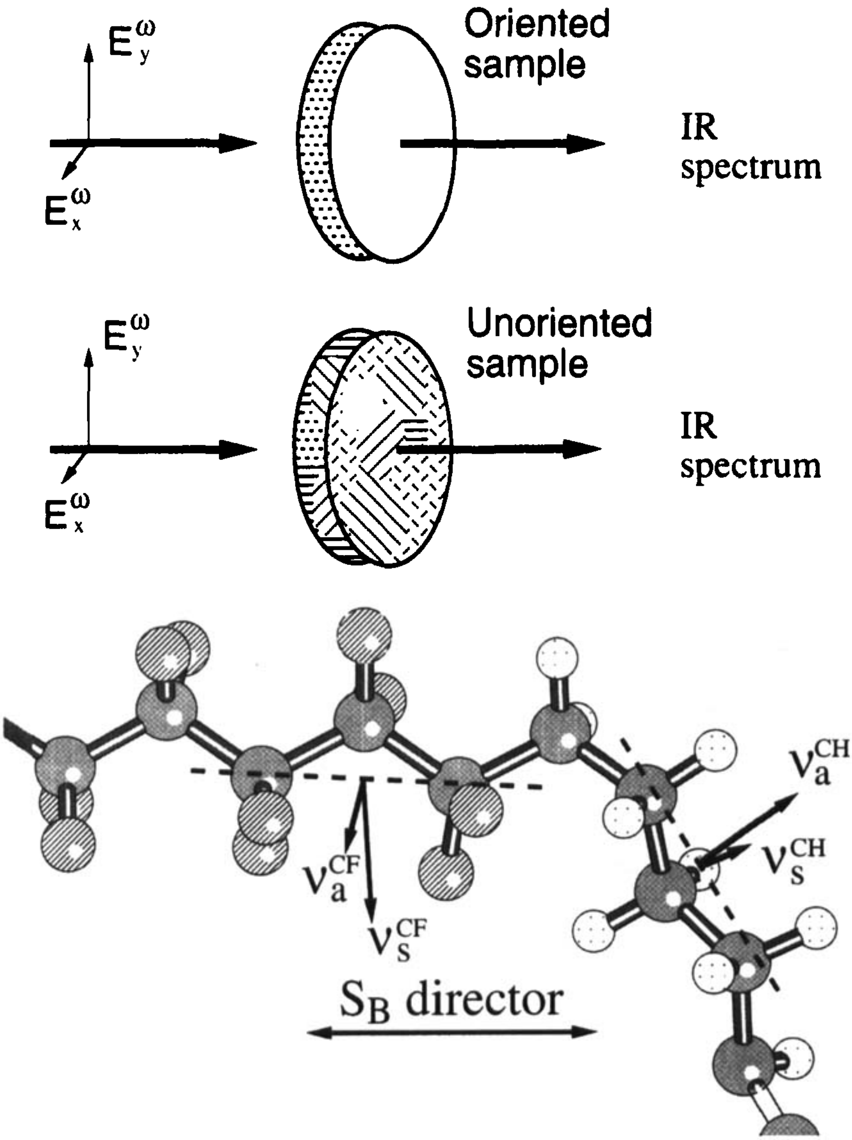

FIGURE 6 Top) Experimental geometry used in infrared dichroism experiments. Bottom) Schematic view showing the polarization of CF_2 and CH_2 stretching modes (ν_s: symmetric, ν_a: antisymmetric)

the regular (isotropic) part of the temperature dependance of the vibrational band intensities was taken into account. The latter was measured on the same substance incorporated in KBr pellets (figure 6a). The apparent order parameter for each oscillator of interest was calculated using the formula:

$$S^* = 1 - \frac{1}{f}\frac{D_h}{D_i} \qquad (6)$$

where f is the thermal correction factor measured from the temperature dependance of band intensities in pellets. S^* permits to calculate the average tilt angle of the oscillator with respect to the layer normal:

$$S^* = \frac{1}{2}(2 - 3\sin^2\theta) \qquad (7)$$

4.2 Results

The infrared spectra of compound C_{10} are presented in figure 7. The bands arising in the 2500–3300 cm^{-1} region correspond to the classical CH_3 and CH_2 stretching modes [30]. The antisymmetric ν_a (2926 cm^{-1}) and symmetric ν_s (2853 cm^{-1}) absorptions are polarized perpendicular to the main chain axis (figure 6b). The stretching vibrations of CH_3 at 2962 and 2853 cm^{-1} are partially overlapped with ν_a and ν_s of CH_2, each absorption pattern recorded in the 2500–3300 cm^{-1} range was decomposed into a sum of lorentzians. The integration of CH_2 ν_a and ν_s bands corrected from their isotropic thermal dependance are plotted in figure 7 for the unoriented and homeotropically oriented samples. The intensities of these bands are practically identical whatever the sample orientation. The order parameter calculated from these data are close to –0.1 (table V) indicating a poor orientation, an order parameter S^* of –0.5 is expected for a perfect homeotropic orientation. This feature is consistent with the picture of molten hydrocarbon chains, as already noticed in solid state NMR experiments [31].

TABLE V Apparent order parameter S^* (7) associated to the CH_2 and CF_2 stretching modes in the smectic B phase of compound C_{10}

	$\bar{\nu}$ *(cm^{-1})*	*43 °C*	*58 °C*	*65 °C (iso)*
CH_2 ν_a	2929	– 0.08	–0.05	0
CH_2 ν_s	2858	–0.13	–0.07	0
CF_2 ν_a	1244	–0.50	–0.46	0
CF_2 ν_s	1152	–0.30	–0.26	0

In the approximation of C_{2v} local symmetry, the antisymmetric ν_a and symmetric ν_s stretching modes of CF_2, both perpendicular to the long chain axis (figure 6b), may be recognized around 1230 and 1149 cm^{-1} respectively [32]. As

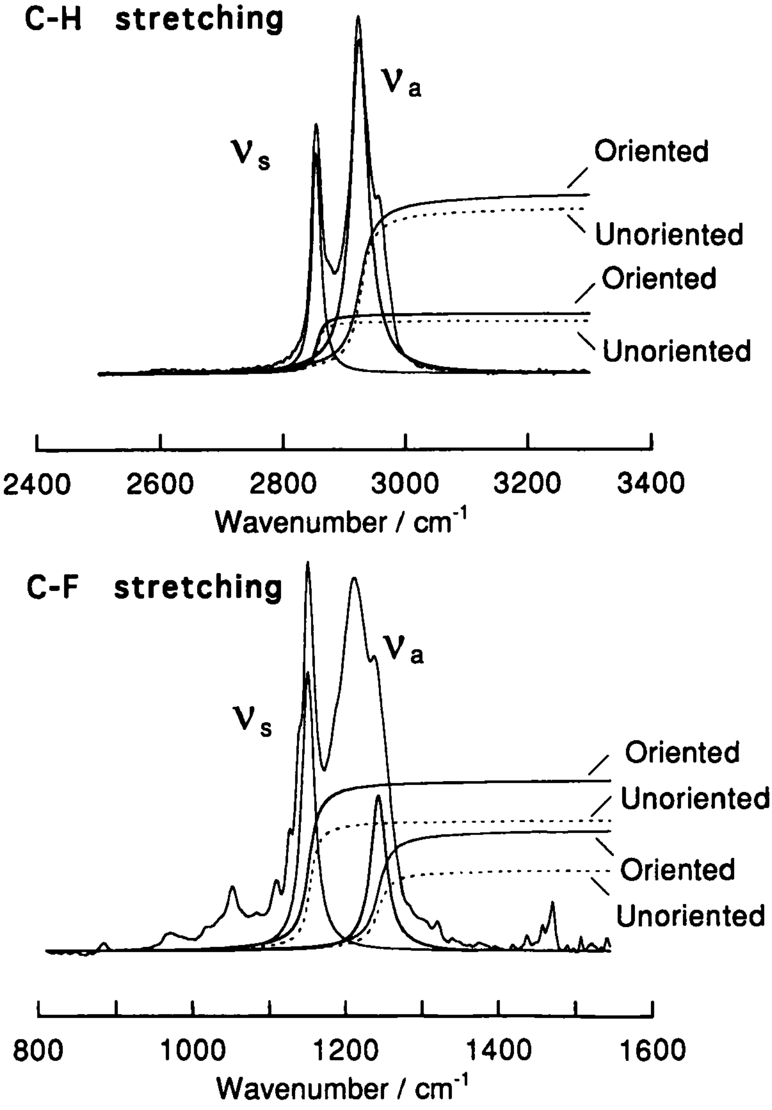

FIGURE 7 Infrared spectra of compound C_{10}. (CF_2 and CH_2 stretching regions). The integration of ν_s and ν_a band amplitudes is shown for oriented and unoriented specimens

previously, these bands are overlapped with strong CF_3 absorptions, their amplitudes were determined after multi-lorentzian decompositions. From the plot of figure 7, it is evident that the intensity of these band is very sensitive to the sample orientation. The apparent order parameter determined from ν_s of CF_2 are close to –0.3 (table V). In the case of ν_a, the apparent order parameter is even stronger, close to the theoretical limit of a perfect homeotropic order (-0.5), but this value should be taken with certain precautions since ν_a in that case is overlapped with a strong CF_3 absorption. The presence of rigid perfluoroalkyl chains perpendicular to the smectic layers together with quasi-molten hydrocarbon chains is in good agreement with the proposed structural model.

5. CONCLUSION

Three different perfluorodecyl-alkane molecules with C_8, C_{10} and a branched C_{11} alkyl parts were synthesized. The structural model proposed for the smectic B phase formed by these molecules is characterized by a segregation of the perfluoroalkyl stems in the middle of the smectic layer. Stretched fluorinated chains are perpendicular to the layer plane and compactly packed. Alkyl chains alternate up and down and fill the remaining space owing to their flexibility. The proposed structural model is in contradiction with the arrangement of tilted interdigitated molecules proposed by Viney et al. [12].

In particular, the segregation of the perfluorinated part of the molecules initially proposed by A. Skoulios et al. [1] is in good agreement with the X-ray diffraction data: *hk*0 reflexions determine the ^{2}D packing and 00*l* intensities are correlated with the electronic density distribution along the direction normal to the layer.

As already seen in smectic E materials [33–34], two different types of conformation are necessary to fulfill the close packing requirements: crystallized rigid stems alternate with quasi-molten flexible chains but in the present case the role of the rigid subunit is played by the perfluoroalkyl chain. The proposed structural model is based on hexagonal packing of fluorinated chains perpendicular to the layer plane. Nevertheless, the monoclinic symmetry deduced from diffraction data suggests an additional in-plane order of the rigid stems.

6. EXPERIMENTAL SECTION

^{13}C and ^1H NMR spectra were recorded using a Brucker AM300 spectrometer in standard conditions. ^{19}F spectra were recorded at 282 MHz from the same device with a resolution of 1.3 Hz/pt. IR spectra were obtained from a Perkin-Elmer 1600 FTIR spectrometer, mass spectra were recorded from a GC-MS setup using a Hewlett-Packard 5971 mass selective detector.

5-ethyl-non-1-ene (7)

2.26 g (94 mmol) of magnesium turnings and 30 mL of anhydrous ether were placed in a 250 mL three necked round bottom flask equipped with magnetic stirrer, reflux condenser and argon inlet. The reaction was started with a few drops of allyl bromide, a crystal of iodine and a gentle heating to bring the mixture to reflux. A solution of 5 mL (29 mmol) of allyl bromide in 10 mL of anhydrous ether was added over 1h30 with stirring. The argon flow was stopped during the addition to avoid excessive solvent evaporation. The reaction mixture was stirred for 20 minutes after the end of the addition. Meanwhile, a solution of 1-bromo-2-ethyl hexane in 10 mL of anhydrous ether was placed in a 250 mL round bottom flask equiped with magnetic stirrer, reflux condenser and argon inlet. A catalytic amount of copper (I) bromide was added and the mixture brought to reflux by gentle heating. The solution of Grignard reagent was then added dropwise to this mixture via the capillary tube over 30 minutes with stirring. The reaction mixture was refluxed for further 30 minutes after the end of the addition, and allowed to stand overnight. 100 g of ice and 10 mL of phosphoric acid were added to this solution and the organic phase extracted twice with ether and once with dichloromethane, then dried over $MgSO_4$. The residue contained almost pure 5-ethyl-non-1-ene, which when purified by vacuum distillation (70°C/26 Torr) produced a colourless liquid. Yield: 65 percent. Analysis found H/C = 0.165 calc H/C = 0.168. IR (NaCl window, cm^{-1}) 3078 (ν_{CH} vinyl), 2961 (ν_a CH_3), 2927 (ν_a CH_2), 2873 (ν_s CH_3), 2860 (ν_s CH_2), 1820 (overtone), 1642 (ν C=C), 1460 (δ CH_2 + δ_a CH_3), 1416 (δ ip $=CH_2$), 1379 (δ_s CH_3), 994, 909 (δ oop =CH), 778, (δ CH_2CH_3), 727 (δ skeletal). MS (impact) 154 M^+, 125 $[C_9H_{17}]^+$, 112 $[C_8H_{16}]^+$, 97 $[C_7H_{13}]^+$, 83 $[C_6H_{11}]^+$, 70 $[C_5H_{10}]^+$, 57 $[C_4H_9]^+$. ^{1}HNMR ($CDCl_3$, δ/ppm, TMS) 5.02 (m, J_3*trans*=16.9 Hz, J_2*gem*=2.2 Hz, J_4=1.5 Hz, 1H, =C*H*H), 4.94 (m, J_3*cis*=10.3 Hz, J_2*gem*=2.2 Hz, J_4=1.1 Hz, 1H, =CH*H*), 5.84 (m, J_3*trans*=16.9 Hz, J_3*cis*=10.3Hz, J_3=6.6Hz, 1H, =C*H*), 2.05 (m, J_3=6.9Hz, J_3=7.5Hz, 2H, =CH-CH_2), 1.27 (br., 11H, CH_2 and CHC_2H_5), 0.92 (t, J_3=6.6 Hz, 3H, $(CH_2)_3$-CH_3), 0.86 (m, J_3=6.6 Hz, J_4= 1.84 Hz, CH_2CH_3). ^{13}CNMR ($CDCl_3$, δ/ppm, TMS) 139.4 (CH_2=), 113.7 (=CH-), 38.2 (CH), 32.6, 32.3, 31.0, 28.8 (CH_2), 25.6 (CH-CH_2-CH_3), 23 (CH_2-CH_2-CH_3), 13.9 (CH_2-CH_2-CH_3). 10.6 (CH-CH_2-CH_3)

15-ethyl-1,1,1,2,2,3,3,4,4,5,5,6,6,7,7,8,8,9,9,10,10-henicosafluoro-12-iodo-nonadecane (mixture of diastereoisomeres) (8)

2.16 g (14 mmol) of 5-ethyl-non-1-ene, 8.1 g (12.5 mmol) of 1 -perfluorodecyl-iodide, and 6 mL heptane were heated at 110°C in a 100 mL three-necked flask. AIBN was added every ten minutes by portions of a few milligrams. After 30 minutes of reaction, NMR analysis indicated the disappearance of vinylic protons. After evaporation of the solvent, the residue was separated by Kugelrohr distillation giving rise to 7.99 g (10 mmol) of the title compound (mp = 50.9°C). Yield: 83 percent. Analysis found C=32.08 H=2.85 calc C=31.52 H=2.77. IR (KBr window, cm^{-1}) 2960 (ν_a CH_3), 2928 (ν_a CH_2), 2874 (ν_s CH_3), 2860 ($\nu_s CH_2$), 1460 (δ CH_2), 1430 (δ_a CH_3), 1370 (δ_s CH_3), 1342 (δ CH), 1243, 1210, 1152 (ν CF), 888 (?), 664, 649 (δ CF_2 and CF_3). ^{1}HNMR ($CDCl_3$, δ/ppm, TMS) 4.34 (m, J_3=7.4Hz, J'_3 = 5.9Hz , 1H, C*HI*), 2.86 (m, 2H, CF_2-CH_2), 1.79 (m, 2H, CHI-CH_2), 1.1–1.6 (11H, C*H* and CH_2), 0.83–0.95 (overlap of triplets, 6H, CH_3). ^{13}CNMR ($CDCl_3$, δ/ppm, TMS) 41.5 (t, J=21.1 Hz, CHI-CH_2-CF_2) 37.9, 38.0 (*C*H), 37.4, 32.8, 32.6, 32.4, 28.8, 28.6 (CH_2), 25.6 (CH-CH_2-CH_3), 22.9 (CH_3-CH_2-$(CH_2)_2$), 21.2 (*C*HI), 13.9 (CH_3-$(CH_2)_3$), 10.6 (CH_2-CH_3). ^{19}FNMR ($CDCl_3$, δ/ppm, $CFCl_3$) −81.4 (t, J_3=9.7 Hz, 3F, CF_3), −112.24 (δ, J_2=270 Hz, 1F, CHI-CF_2-CF*F*), −115.2 (δ, J_2=270 Hz, 1F, CHI-CF_2-C*F*F),-122.4 (10F, CF_2), −123.3 (2F, CF_2), −124.1 (2F, CF_2), −126.7 (2F, CF_2-CF_3)

1,1,1,2,2,3,3,4,4,5,5,6,6,7,7,8,8,9,9,10,10-henicosafluoro-12-iodo-octadecane (3a)

Was prepared similarly from perfluorodecyl iodide and 1-octene. The product was used in the next step without purification. Yield: 66 percent. IR (KBr window, cm^{-1}) 2959 (ν_a CH_3), 2927 (ν_a CH_2), 2875 (ν_s CH_3), 2857 (ν_s CH_2), 1466 (δ CH_2), 1377 (δ_s CH_3), 1342 (δ CH), 1244, 1220, 1152 (ν CF), 724 (δ CH_2). MS (impact), 219 $[C_4F_9]^+$, 183 $[C_4H_8I]^+$, 181 $[C_4F_7]^+$, 169 $[C_3H_6I]^+$, 155 $[C_2H_4I]^+$, 141 $[CH_2I]^+$, 131 $[C_3F_5]^+$, 127 $[I]^+$, 119 $[C_2F_5]^+$, 91 $[C_7H_7]^+$, 71 $[C_5H_{11}]^+$, 69 $[CF_3^+]$, 57 $[C_4H_9]^+$, 55 $[C_4H_7]^+$. ^{1}HNMR ($CDCl_3$, δ/ppm, TMS) 4.5 (m, 1H, C*HI*), 3 (m, 2H, CF_2-CH_2), 1.8 (m, 2H, CHI-CH_2), 1.2 (CH_2), 0.85 (t, 3H, CH_3).

1,1,1,2,2,3,3,4,4,5,5,6,6,7,7,8,8,9,9,10,10-henicosafluoro-12-iodo-eicosane (3b)

Was prepared similarly from perfluorodecyl iodide and 1-decene. The compound was purified by kugelrohr distillation. Yield 63 percent. ^{1}HNMR ($CDCl_3$, δ/ppm, TMS) 4.34 (m, 1H, C*HI*), 2.85 (m, 2H, CF_2-CH_2), 1.81 (m, 2H, CHI-CH_2), 1.54, 1.3 (CH_2), 0.87 (CH_3). ^{13}CNMR ($CDCl_3$, δ/ppm, TMS) 41.5 (t, J=20.8 Hz, CH_2-CF_2), 40.18, 40.20 (CH_2-CH_2-CHI), 31.65 (CH_3-CH_2-CH_2), 29.4, 29.2, 29.0, 28.3 (CH_2), 20.7 (*C*HI), 22.5 (CH_3-CH_2), 13.9 (CH_3).

15-ethyl-1,1,1,2,2,3,3,4,4,5,5,6,6,7,7,8,8,9,9,10,10-henicosafluorononadecane (racemic) (9; C_{11}^*)

1.57g (1.96 mmol) of 15-ethyl-1,1,1,2,2,3,3,4,4,5,5,6,6,7,7,8,8,9,9,10,10-henicosafluoro-12-iodo-nonadecane were placed in a 500 mL three necked flask, together with 1g of zinc powder, 85 mL of *iso*-octane and 50 mL of propanol. The flask was fitted with a reflux condenser and immersed into an oil bath at 110°C. Gaseous HCl was bubbled into the solution for two hours with stirring. The mixture was cooled down and filtered. The solvent was evaporated under vacuum and cold water was added. The compound precipitated at the cold. The crude waxy solid was redissolved in CH_2Cl_2, thoroughly washed with distilled water, dried over $MgSO_4$. After evaporation of the solvent, the compound was purified by Kugelrohr distillation and obtained as a colourless waxy solid (865 mg). Recrystallization in a methanol-acetone mixture (1:3) afforded 605 mg. Yield: 46 percent. Analysis found C=37.93 H=3.54 calc C=37.40 H=3.44. IR (KBr window, cm^{-1}) 2961 (ν_a CH_3), 2928 (ν_a CH_2), 2874 (ν_s CH_3), 2862 (ν_s CH_2), 1466 (δ CH_2), 1375 (δ CH_3), 1342 (?), 1241, 1210, 1152 (ν CF), 1111, 1080, 900, 882, 706 (?), 666, 648 (δ CF_2 and CF_3). ^{1}HNMR ($CDCl_3$, δ/ppm, TMS). 2.07 (m, 2H, CF_2-CH_2), 1.60 (m, 2H, CF_2-CH_2-CH_2), 1.42–1.19 (*CH* and CH_2), 0.91 (t, 3H, J=6.8 Hz, CH_2-CH_3) 0.85 (t, 3H, J=7.2 Hz, $(CH_2)_3$-CH_3). ^{13}CNMR ($CDCl_3$, δ/ppm, TMS) 38.5(CH), 30.8 (t, J_2CF=22.15 Hz, CF_2-CH_2), 32.64, 32.63, 26.1 (CH_2), 28.8 (CH_2-CH_2-CH_3), 25.6 (CH-CH_2-CH_3), 22.9 (CH_2-CH_2-CH_3), 20.4 (CF_2-CH_2-CH_2), 13.9 ($(CH_2)_3$-CH_3), 10.6 (CH_2-CH_3). ^{19}FNMR ($CDCl_3$, δ/ppm, $CFCl_3$) −81.4 (t, J_3=9.7 Hz, 3F, CF_3), −114.9 (2F, CH_2-CF_2-CF_2), −122.3 (10F, CF_2), −123.2 (2F, CF_2), −124.1 (2F, CF_2), −126.7 (2F, CF_2-CF_3).

1,1,1,2,2,3,3,4,4,5,5,6,6,7,7,8,8,9,9,10,10-henicosafluorooctadecane (4a; C_8)

Was prepared similarly from compound **3a**. IR (KBr window, cm^{-1}) 2959 (ν_a CH_3), 2930 (ν_a CH_2), 2860 (ν_s CH_2), 1467 (δ CH_2), 1378 (δ CH_3), 1242, 1213, 1152 (ν CF), 725 (δ CH_2), 666, 642 (δ CF_2 and CF_3). MS (impact), (319, 269, 219, 169, 119, 69) $[C_nF_{2n+1}]^+$, (481, 431, 381, 331, 281, 231, 181, 131) $[C_nF_{2n-1}]^+$, (495, 445, 395, 345) $[C_nF_{2n-3}H_2]^+$, (477, 427, 377) $[C_nF_{2n-4}H_3]^+$, 100 $[C_2F_4]^+$, 91 $[C_7H_7]^+$, 85 $[C_6H_{13}]^+$, 71 $[C_5H_{11}]^+$, 57 $[C_4H_9]^+$, 55 $[C_4H_7]^+$. ^{1}HNMR ($CDCl_3$, δ/ppm, TMS) 2.05 (m, 2H, CF_2-CH_2), 1.60 (m, 2H, CF_2-CH_2-CH_2), 1.42–1.19 (10H, CH_2), 0.89 (t, 3H, J=6.8 Hz, CH_3). ^{13}CNMR ($CDCl_3$, δ/ppm, TMS) 31.71 (CH_2-CH_2-CH_3). 30.87 (t, J_2CF=22.6 Hz, CF_2-CH_2), 29.14, 29.08, 29.00 (CH_2), 22.57 (CH_2-CH_3), 20.04 (t, J_3CF=3.7 Hz, CF_2-CH_2-CH_2), 13.96 (CH_3).

1,1,1,2,2,3,3,4,4,5,5,6,6,7,7,8,8,9,9,10,10-henicosafluoroeicosane (4b; C_{10})

Was prepared similarly from compound **3b**. IR (KBr window, cm^{-1}) 2961 (ν_a CH_3), 2928 (ν_a CH_2), 2876 (ν_s CH_3), 2858 (ν_s CH_2), 1472 (δ CH_2), 1374 (δ CH_3),1240, 1216, 1154 (ν CF), 724 (δ CH_2), 662, 644 (δ CF_2 and CF_3). MS (impact), (531, 481, 431, 381, 331, 281, 231, 181, 131) $[C_nF_{2n-1}]^+$, (269, 219, 169, 119, 69) $[C_nF_{2n+1}]^+$, (495, 445, 395) $[C_nF_{2n-3}H_2]^+$, (477, 427) $[C_nF_{2n-4}H_3]^+$, 99 $[C_7H_{15}]^+$, 85 $[C_6H_{13}]^+$, 71 $[C_5H_{11}]^+$, 57 $[C_4H_9]^+$, 55 $[C_4H_7]^+$. ^{1}HNMR ($CDCl_3$, δ/ppm, TMS) 2.05 (m, 2H, CF_2-CH_2), 1.61 (m, 2H, CF_2-CH_2-CH_2), 1.42–1.19 (14H, CH_2), 0.90 (t, 3H, J=6.6 Hz, CH_3). ^{13}CNMR ($CDCl_3$, δ/ppm, TMS) 31.80 (CH_2-CH_2-CH_3), 30.83 (t, J_2CF=22.6 Hz, CF_2-CH_2), 29.46, 29.23, 29.34, 29.18, 29.07 (CH_2), 22.58 (CH_2-CH_3), 20.00 (t, J_3CF=3.7 Hz, CF_2-CH_2-CH_2), 13.82 (CH_3).

Acknowledgements

We are grateful to Nicolas Lequeux for his help in experiments using the position sensitive detector, Colette Jallabert and Jacqueline Canny are thanked for NMR analyses.

References

1. Mahler, W.; Guillon, D.; Skoulios, A. *Mol. Cryst. Liq. Cryst. Letters* **1985**, *2*, 111.
2. Hildebrand, J. H.; Scott, R. L. *Regular Solution* (Prentice Hall, Englewood, New Jersey 1962).
3. Janulis, E. P.; Novack, J. C.; Papapolymerou, G. A.; Tristani-Kendra, M.; Huffman, W., A. *Ferroelectrics* **1988**, *85*, 375.
4. Nguyen, H.T.; Sigaud, G.; Achard, M. F.; Hardouin, F.; Twieg, R. J. Betterton, K.; *Liquid Crystals* **1991**, *3*, 389.
5. Twieg, R.; Betterton, K.; DiPietro, R.; Gravert, D.; Nguyen, C.; Nguyen, H. T.; Babeau, A.; Destrade, C. *SPIE Proceedings* **1991**, *1455*, 86.
6. Pausch, A. E.; Finkenzeller, U.; Poetsch, E.; Waechtler, A. E. F.; Reiffenrath, V. *International Liquid Crystal Conference (Freiburg 1992).*
7. Volkov, V.V.; Platé, N.A.; Takahara, A.; Kajiyama, T.; Amaya, N.; Murata, Y. *Polymer* **1992**, *33*, 1316.
8. Höpken, J.; Möller, M.; Lee, M.; Percec, V. *Makromol. Chem.* **1992**, *193*, 275.
9. Shimizu, T.; Tanaka, Y.; Kutsumizu, S.; Yamo, S. *Makromol. Symp.* **1994**, *82*, 173.
10. Wang, J.; Mao, G.; Ober, C.K.; Kramer, E.J. *Macromolecules* **1997**, *30*, 1906.
11. Tournilhac, F.; Simon, J.; Nicoud, J. F.; Bosio, L. *Chem. Phys. Letters* **1988**, *145*, 452.
12. Viney, C.; Russel, T.P.; Depero, L.E.; Twieg, R.J. *Mol. Cryst. Liq. Cryst.* **1988**, *165*, 317.
13. Tamura, M.; Kochi, J.; *J. Am. Chem. Soc.* **1971**, *93*, 1485.
14. Haszeldine, R.N. *J. Chem. Soc.* 1949, 2856.
15. Brace, N.O.; *J. Org. Chem.* **1962**, *27*, 3033.
16. Brace, N.O.; *J. Org. Chem.* **1962**, *27*, 4491.
17. Clark, T. *Hydrocarbons* in *Comprehensive Organic Chemistry* Barton, D.; Ollis, W.D. Ed. Pergamon Oxford 1979.
18. de Santis, P.; Giglio, E.; Liquori, A.M.; Ripamondi, A. *J. Polym. Sci.* **1963**, *A1*, 1383.
19. Kitaigorodsky, A.I. *Molecular Crystals and Molecules* Academic Press London 1973.
20. Cense, J.M. *Moldraw* Software, Ecole Nationale Supérieure de Chimie, Paris 1993.
21. Mita, S.; Fujiwara, M.; Kondo, S. *Mol. Cryst. Liq. Cryst.* **1999**, *330*, 1281.

22. Skoulios, A. *Adv. Colloïd Interface Sci.* **1967**, *1*, 79.
23. Bunn, C.W.; Howells, E.R. *Nature* **1954**, *174*, 549.
24. Clark, E.S.; Muus, L.T. *Z. Krist.* **1962**, *117*, 119.
25. Dorset, D.L. *Chem. and Phys. of Lipids* **1977**, *20, 13*.
26. Kromm, P. *Thesis* Bordeaux (1995); Kromm, P.; Cotrait, M.; Nguyen, H.T. *Liq. Cryst.* **1996**, *21*, 95.
27. Höpken, J.; Möller, M. *Macromolecules* **1992**, *25*, 2482.
28. Caillé A. *C. R. Acad. Sci Paris* **1972**, *B274*, 891.
29. Blinov, L.M.; Tournilhac, F. *Mol. Cryst. Liq. Cryst. Sci. Tech. Sec. C* **1993**, *3*, 93.
30. George, W.O.; McIntyre P.S. *Infrared spectroscopy* Wiley Chichester 1987.
31. Höpken, J.; Pugh, C.; Richtering, W.; Möller, M. *Makromol. Chem.* **1988**, *189*, 911.
32. Liang, C.Y.; Krimm, S. *J. Appl. Phys.* **1956**, *25*, 563.
33. Pensec, S.; Tournilhac, F.G.; Bassoul, P. *J. Phys. II (France)* **1996**, *6*, 1597.
34. Pensec, S.; Tournilhac, F.G.; Bassoul, P.; Durliat C. *J. Phys. Chem. B.* **1998**, *102*, 52.